IEEE Access
Multidisciplinary ⋮ Rapid Review ⋮ Open Access Journal

Received 3 October 2023, accepted 12 October 2023, date of publication 17 October 2023, date of current version 30 October 2023.

Digital Object Identifier 10.1109/ACCESS.2023.3325294

RESEARCH ARTICLE

RU-Net2+: A Deep Learning Algorithm for Accurate Brain Tumor Segmentation and Survival Rate Prediction

RUQSAR ZAITOON AND HUSSAIN SYED
School of Computer Science and Engineering, VIT-AP University, Amaravati, Andhra Pradesh 522237, India
Corresponding author: Hussain Syed (hussain.syed@vitap.ac.in)

ABSTRACT Brain tumors present a significant medical concern, posing challenges in both diagnosis and treatment. Deep learning has emerged as an evolving technique for automating the diagnostic process for brain tumors. This research paper introduces a novel deep-learning framework designed explicitly for brain tumor diagnosis. The framework encompasses various tasks: tumor detection, classification, segmentation, and survival rate prediction. The framework was applied to the BraTS dataset, an extensive collection of brain tumor images, to evaluate its effectiveness. The proposed workflow initiates with data acquisition, followed by an enhancement of this data using a Convolutional Normalized Mean Filter (CNMF) during pre-processing. This prepares the data for the multi-class classification performed using the novel DBT-CNN classifier model. The RU-Net2+ model is employed for precise tumor demarcation, yielding segmented regions from which features are subsequently extracted utilizing the Cox model. These extracted features play a pivotal role in the final step, where the survival rate of patients is predicted using a logistic regression model. The experimental results showcased the exceptional performance of the proposed framework, surpassing current benchmarks in classification accuracy, tumor segmentation precision, and survival rate prediction. For high-grade glioma (HGG) tumors, the framework achieved an impressive classification accuracy of 99.51%, while for low-grade glioma (LGG) tumors, the accuracy reached 99.28%. The accuracy of tumor segmentation stood at 98.39% for HGG tumors and 99.1% for LGG tumors. The RU-Net2+ algorithm accurately predicts patient survival rates: 85.71% long-term, 72.72% medium-term, and 61.54% short-term, with corresponding Mean Squared Errors of 0.13, 0.21, and 0.31. These results provide valuable insights for medical professionals making brain tumor treatment decisions. Additionally, the framework shows promise for automating brain tumor diagnosis and enhancing patient care.

INDEX TERMS Brain tumor, MRI images, deep learning, machine learning, CNMF, RU-Net2+, DBT-CNN, BraTs.

I. INTRODUCTION

Brain tumors pose a significant health concern and can cause severe patient consequences. It is crucial to promptly and precisely diagnose brain tumors to facilitate effective treatment strategies [1]. The conventional approaches to segmenting, classifying, and predicting the risks associated with brain tumors have encountered limitations in accuracy and efficiency. Deep learning-based models have recently emerged as powerful tools in medical imaging analysis [2]. These models can significantly improve the accuracy and efficiency of brain tumor diagnosis. However, significant challenges hinder their effective deployment in clinical settings. These challenges include data quality and availability, computational complexity, inter-modality variations, model generalization, overfitting, interpretability, temporal dynamics, annotation, labeling issues, integration into clinical workflows, and ethical considerations, including data privacy and biases [3].

In this environment, there's a pressing requirement for an advanced deep learning model that can adeptly and precisely

The associate editor coordinating the review of this manuscript and approving it for publication was Zhan-Li Sun.

handle the segmentation, classification, and risk prediction of brain tumors. The model must be robust to variations in data, capable of handling high-dimensional data, and adept at capturing intricate tumor structures. Furthermore, it should be interpretable, scalable, and easily integrated into clinical workflows. Addressing these requirements is essential for providing timely and effective care to patients with brain tumors.

The motivation behind this research is multifold. First, there is an imperative need to improve the early detection and accurate classification of brain tumors, which can significantly enhance patients' prognosis and quality of life. Second, developing more sophisticated models to treat a multiclass variety of tumors is needed. Additionally, reducing the computational costs associated with these models is necessary to make them more accessible and feasible in clinical settings [4]. Finally, predicting patient outcomes and survival rates can be invaluable for personalized treatment plans.

The Brain Tumor Segmentation (BraTS) dataset [5] is a vital resource in the research community, comprising a diverse range of multimodal magnetic resonance imaging (MRI) scans for the detection, segmentation, and classification of brain tumors. It offers high-quality, anonymized, standardized data, ideal for various applications, including deep learning models for brain tumor analysis. The dataset embraces multiple MRI modalities such as T1, T1Gd (T1 post-contrast gadolinium-enhanced), T2, and T2-FLAIR (T2 Fluid Attenuated Inversion Recovery), each contributing unique tumor characteristics for a comprehensive analysis. Expert annotations encapsulate the tumor's entirety, core, and enhancing regions, enabling detailed multiclass segmentation tasks. These features form the foundation for the deep learning-based multimodal diagnosis model. This advanced technique leverages the rich multimodal data in BraTS for efficient brain tumor segmentation, classification, and risk prediction. The model, powered by the multi-faceted view of the tumor offered by the diverse MRI scans, significantly bolsters the diagnostic capability compared to unimodal approaches [6].

Recent studies in [38] and [39] have highlighted the growing potential of integrated deep learning frameworks, which not only focus on tumor detection but also extend their capabilities to segmentation, classification, and even survival rate prediction. These advancements raise pertinent questions:

1. *Creating a Comprehensive Multimodal Diagnosis Model:* How can we develop a comprehensive deep learning-based multimodal diagnosis model capable of simultaneous and precise execution of segmentation, classification, and risk prediction for brain tumors?
2. *Innovative Pre-processing Techniques*: Can innovative pre-processing techniques, such as CNMF, significantly enhance the accuracy and efficiency of brain tumor diagnosis when combined with state-of-the-art segmentation and classification models?
3. *Comparative Effectiveness and Computational Efficiency:* How does the proposed approach compare in terms of effectiveness and computational efficiency with the recent advancements in this field?

To address these questions, this study introduces a deep-learning framework designed specifically for brain tumor diagnosis. This framework not only aims to detect and segment tumors but also classifies them and predicts patient survival rates. This comprehensive approach could be pivotal in advancing the capabilities of automated diagnostic tools, ensuring that medical professionals receive timely and accurate information critical for patient care.

This research aims to develop a comprehensive deep learning-based multimodal diagnosis model for brain tumor segmentation, classification, and risk prediction. The model will integrate multiple imaging modalities for enhanced feature extraction. It will utilize advanced preprocessing techniques like CNMF [7] to address data quality and inter-modality variations. It will employ sophisticated algorithms such as RU-Net2+ for precise segmentation and DBT-CNN for detailed classification. Incorporating risk prediction algorithms like the multivariate Cox model and logistic regression will enable prognostic insights. Moreover, the research will emphasize ensuring model interpretability, rigorous performance evaluation on diverse datasets, adherence to ethical standards, including data privacy, and developing a user-friendly interface for seamless clinical integration, all aiming toward improved diagnostic accuracy and patient outcomes. The contribution of the research work can be summarized point-wise as follows

- Developed a novel framework for brain tumor analysis that integrates detection, segmentation, classification, and patient risk prediction.
- Incorporated the Cox multivariate model for survivability prediction based on extracted features.
- Implemented a specialized RU-Net2+ model for precise tumor segmentation and optimized the framework to improve accuracy, robustness, and computational efficiency.
- Evaluated the framework's effectiveness in improving brain tumor diagnosis and treatment.

The rest of the paper is organized as, section II presents the related work, section III describes the proposed methodology in detail i.e., image acquisition, pre-processing, segmentation, classification of brain tumor, and patient prediction risk. Performance measures and experimental requirements are discussed in section IV, and results and comparative analysis are provided in section V. Section VI concludes the work and describes future work.

II. RELATED WORK

In recent years, there has been a growing interest in the use of deep learning for brain tumor segmentation and classification. A number of different approaches have been proposed, including:

Deep convolutional neural networks (CNNs) have been used for both segmentation and classification tasks. CNNs are able to learn the spatial relationships between different features in images, which make them well-suited for tasks such as tumor segmentation. Hybrid approaches that combine CNNs with other machine learning methods have also been proposed. These approaches can often achieve better performance than CNNs alone. Ensemble methods that combine the predictions of multiple models have also been shown to be effective for brain tumor segmentation and classification.

The following are some of the recent papers that have proposed novel methods for brain tumor segmentation and classification using deep learning:

Brain tumors are a major cause of cancer-related death worldwide. Early diagnosis and treatment of brain tumors is essential for improving patient outcomes. In recent years, deep learning has emerged as a powerful tool for brain tumor segmentation and classification.

Several recent studies have applied deep learning to brain tumor segmentation and classification. In [8], a novel adaptive eroded deep convolutional neural network (AEDCNN) was proposed for brain image segmentation and classification. The AEDCNN was used to segment the tumor region from brain images, and then the Inception ResnetV2 model was used to classify the tumor as benign or malignant. The AEDCNN was able to provide distinct segmentation between meningioma, glioma, and pituitary brain regions. The Inception ResnetV2 model was able to achieve an accuracy of 97.89% and a precision of 93.27% for tumor classification.

Another recent study, [9], proposed a hybrid deep convolutional neural network (CNN) with Nature-inspired ResNet 152 Transfer Learning (Hyb-DCNN-ResNet 152 TL) model for brain tumor detection and classification. The Hyb-DCNN-ResNet 152 TL model was able to achieve an accuracy of 99.57%, 97.28%, 94.31%, 95.48%, 96.38%, 98.41%, and 96.34% for tumor detection and classification.

A hybrid algorithm for brain tumor segmentation, classification, and feature extraction was proposed in [10]. The algorithm uses threshold segmentation and the watershed algorithm for tumor segmentation, and then different classifiers are used for tumor classification. The algorithm was able to achieve an accuracy of 90% for tumor classification.

A semantic segmentation method for brain tumor prediction using deep learning was proposed in [11]. The method uses a convolutional neural network to segment the tumor region from brain images, and then the tumor region is classified as benign or malignant. The method was able to achieve an accuracy of 91.718% for tumor prediction.

A method for 3D brain tumor segmentation and survival prediction using ensembles of convolutional neural networks (CNNs) was proposed in [12]. The method uses an ensemble of asymmetric U-Net-like architectures for tumor segmentation and a DenseNet model for survival prediction. The method was able to achieve a dice score of 0.82 for tumor segmentation and an accuracy of 0.57 for survival prediction.

A triple-intersecting U-Net (TIU-Net) for brain glioma segmentation was proposed in [13]. The TIU-Net is composed of binary-class segmentation U-Net (BU-Net) and multi-class segmentation U-Net (MU-Net), in which MU-Net reuses multi-resolution features from BU-Net. The BU-Net predicts a segmentation soft mask, which is used to generate candidate glioma regions that are then segmented by the MU-Net. An edge branch in the MU-Net is used to enhance boundary information, which helps to improve segmentation accuracy. The TIU-Net was evaluated on the BRATS 2015 dataset and achieved state-of-the-art results.

A new method for segmenting brain tumors in MRI images and classifying them into tumor stages was proposed in [14]. The method uses a weighted fuzzy clustering algorithm, a deep auto-encoder (DAE), a barnacle mating algorithm (BMOA), and a random forest (RF) classifier. The DAE is used to extract features from the MRI images, the BMOA is used to cluster the features, and the RF classifier is used to classify the tumor stages. Experimental results on the BRATS 2015 dataset showed that the proposed method achieves high accuracy in tumor segmentation and classification.

A new method for classifying brain tumors based on an improved version of the whale optimization algorithm (WOA) was proposed in [15]. The WOA is a meta-heuristic algorithm that is used to optimize the parameters of a classifier. The proposed method uses the WOA to optimize the parameters of a multilayer perceptron (MLP) classifier. Experimental results on the BRATS 2015 dataset showed that the proposed method achieves high accuracy in brain tumor classification.

A context-aware deep learning approach for brain tumor segmentation, subtype classification, and survival prediction was proposed in [16]. The approach uses a 3D context-aware deep learning model to segment tumors, a regular 3D CNN to classify tumor subtypes, and a hybrid deep learning and machine learning method to predict survival. Experimental results on the BRATS 2019 and CPM-RadPath 2019 datasets show that the proposed approach achieves state-of-the-art performance in tumor segmentation, subtype classification, and survival prediction.

A new semantic segmentation method for brain tumor prediction using deep learning [11]. The method uses a convolutional neural network (CNN) to predict the location and extent of brain tumors in 3D. The CNN is trained on a dataset of 3D brain MRI images. Experimental results on the BRATS 2015 dataset show that the proposed method achieves high accuracy in brain tumor prediction.

A dynamic architecture-based deep learning approach for glioblastoma brain tumor survival prediction [17]. The approach uses a combination of MRI images, radiomic features, and machine learning algorithms to predict the survival of patients with glioblastoma. The approach was evaluated on a dataset of 100 patients and achieved an accuracy of 95%.

A method for brain tumor segmentation using an ensemble of 3D U-Nets and overall survival prediction using

TABLE 1. Summary of brain tumor segmentation and classification studies.

reference	Method	Dataset Used	Tumor Segmentation Accuracy	Tumor Classification Accuracy	Survival Prediction Accuracy
[8]	AEDCNN + Inception ResnetV2	N/A	Distinct segmentation	97.89%	N/A
[9]	Hyb-DCNN-ResNet 152 TL	N/A	N/A	99.57%	N/A
[10]	Hybrid algorithm	N/A	N/A	90%	N/A
[11]	CNN	N/A	91.718%	N/A	N/A
[12]	Ensemble of CNNs	N/A	0.82 (Dice score)	N/A	0.57
[13]	TIU-Net	BRATS 2015	State-of-the-art results	N/A	N/A
[14]	Weighted fuzzy clustering + DAE + BMOA + RF	BRATS 2015	High accuracy	High accuracy	N/A
[15]	Improved WOA + MLP classifier	BRATS 2015	N/A	High accuracy	N/A
[16]	3D context-aware deep learning model + 3D CNN + hybrid deep learning and machine learning	BRATS 2019, CPM-RadPath 2019	State-of-the-art performance	State-of-the-art performance	State-of-the-art performance
[17]	CNN	BRATS 2015	High accuracy	N/A	N/A
[18]	Combination of MRI images, radiomic features, and machine learning algorithms	100 patient dataset	N/A	N/A	95%
[19]	Ensemble of 3D U-Nets + radiomic features	BraTS 2018	91%	N/A	82%
[20]	CNN	BraTS 2017	91%	N/A	N/A
[21]	Multimodal deep-learning framework	Two patient cohorts	N/A	N/A	82% (adult), 75% (pediatric)

radionics features [18]. The approach uses a combination of MRI images, 3D U-Nets, and radiomic features to segment brain tumors and predict patient survival. The approach was evaluated on the BraTS 2018 dataset and achieved an accuracy of 91% for tumor segmentation and 82% for patient survival prediction.

A brain tumor segmentation method based on deep learning's feature representation [19]. The approach uses a convolutional neural network to extract features from MRI images and then uses these features to segment the tumor. The approach was evaluated on the BraTS 2017 dataset and achieved an accuracy of 91% for tumor segmentation.

A multimodal deep-learning framework to predict prognosis in adult and pediatric brain tumors [20]. The framework fuses histopathology images with gene expression profiles to predict patient survival. The framework was evaluated on two cohorts of patients and achieved an accuracy of 82% for adult patients and 75% for pediatric patients.

The mentioned research work highlights various issues and concerns pertaining to the segmentation, classification, and risk prediction of brain tumors using deep learning techniques. These challenges encompass the variability of data, the ability of models to generalize, the accuracy of segmentation, the performance of classification, the prediction of survival rates, the interpretability of results, the integration of multiple modalities, the computational and resource requirements, ethical considerations, and the validation of the proposed model in real-world clinical scenarios. The proposed work must address these challenges comprehensively to ensure the utilization of representative and diverse datasets, mitigate the risk of overfitting, enhance the accuracy of segmentation and classification, improve the prediction of survival rates, provide interpretability of the model's outputs, integrate information from various modalities, optimize computational efficiency, adhere to ethical guidelines, and validate the effectiveness of the model in real-world clinical settings. Successfully overcoming these challenges will contribute significantly to the development of a robust and practical deep learning-based multimodal diagnostic model for the analysis of brain tumors.

III. MATERIAL AND METHODS

The brain is a complex organ that governs every process of the human body thinking, sensibility, remembrance, recall, affection, manual skills, touch, vision, imagination, desire, and every other process. Therefore, even minor damage, illness, or other issues to the brain could have a devastating effect on a person's life. They are several brain and nervous system diseases and disorders caused due to certain issues that need to be diagnosed in the primary stage since it is a complex organ that cannot be properly diagnosed and treated in advanced stages. Among all brain diseases, the most caused

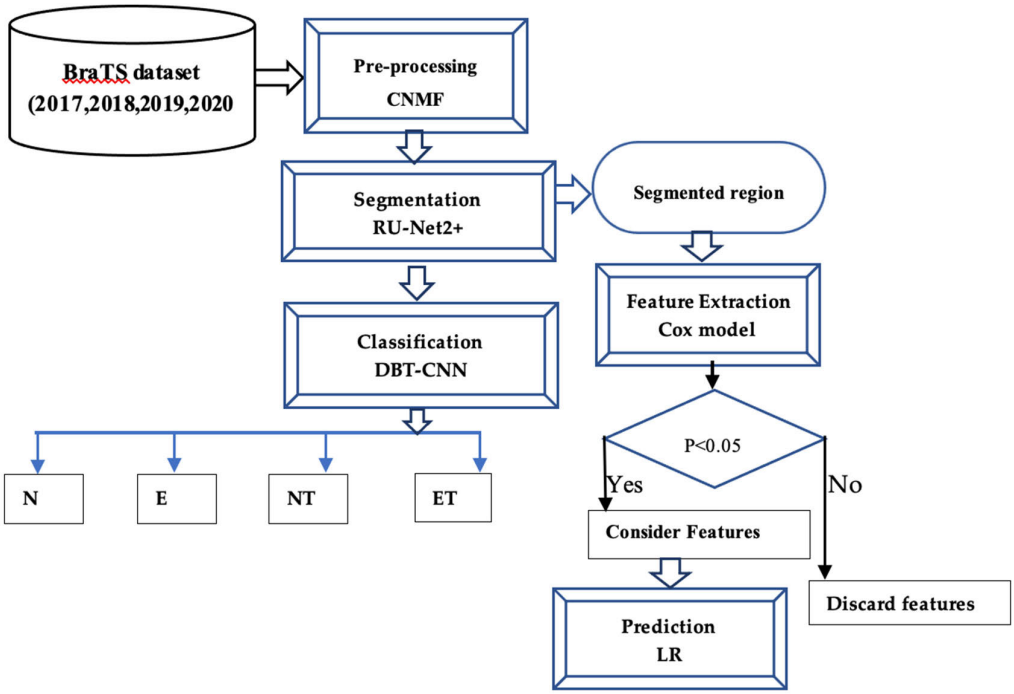

FIGURE 1. Proposed model architecture for brain tumor diagnosis.

disease is a brain tumor, the growth, and formation of mass in the brain due to abnormal cell activity. They are various forms of brain tumors mainly classified into two types based on their effect benign (non-cancerous) and malignant (cancerous). It can also be classified based on the tumor origin i.e., primary (growth in the brain) and metastatic tumors (spread from other parts). The development of brain tumors can vary significantly; the growth rate and location of the tumor specify the effect on brain functioning. The diagnosis depends on the tumor location/region, size, and type, location therefore, early and precise detection of the tumor is necessary to save the patient's life. The traditional methods usually fail in the precise location and segmentation of the tumor, to address this problem a computer-aided diagnosing model is proposed to identify, segment, and classify the tumor accurately in the primary stage, and to predict the survival rate of patients as shown in figure 1.

A. DATASET

In this study, we utilized the publicly available BraTS dataset, comprising multimodal MRI scans of brain tumors. Specifically, we employed the BRATS datasets from 2017 [40], 2018 [21], 2019 [22], and 2020 [23] which are recognized for their effectiveness in deep learning applications. These datasets encompass two prevalent types of brain tumors, High-Grade Glioma (HGG) and Low-Grade Glioma (LGG), along with four distinct MRI scan modalities: T1 (Tissue - longitudinal relaxation time), T1C (T1 Contrast), T2 (tissue transverse relaxation time), and FLAIR (Fluid Attention Recovery). For our experiments, we allocated 70% of the data for training and the 20% for testing and remaining 10% for validation. Detailed dataset information can be found in Table 2, and sample MRI scans from the BraTS dataset are illustrated in Figure 3. The Brain Tumor Segmentation (BraTS) dataset has been a cornerstone in the brain tumor research community along with the subsequent versions, consists of multimodal MRI scans that capture different characteristics of brain tumors.

To elaborate on the four MRI modalities used:

1. **T1 (Tissue - longitudinal relaxation time)**: Provides detailed anatomical views of the brain and is particularly useful in identifying changes in brain tissue.
2. **T1C (T1 Contrast)**: A contrast-enhanced T1 image, making abnormalities more apparent and aiding in discerning them from the surrounding healthy tissues.
3. **T2 (tissue transverse relaxation time)**: Highlights certain differences between normal and abnormal tissues, particularly useful for detecting edema (fluid) and inflammations.
4. **FLAIR (Fluid Attenuated Inversion Recovery)**: Helps in identifying lesions filled with fluid, providing a more accurate depiction of brain tumors.

The combination of these four modalities ensures a comprehensive understanding of brain tumors, from their location and extent to their interaction with surrounding tissues.

B. IMAGE PRE-PROCESSING

In the medical image analysis domain, image pre-processing is the crucial step, since the images consist of artifacts, noise,

TABLE 2. Detail description of datasets, the total number of patients, images, and LGG, HGG cases.

Dataset Name	No. of patients	Total Images	HGG	LGG
BraTS'17	285	885	580	275
BraTS'18	266	798	500	298
BraTS'19	285	855	510	345
BraTS'20	335	1005	755	250
Total		3,513	2,345	1,168

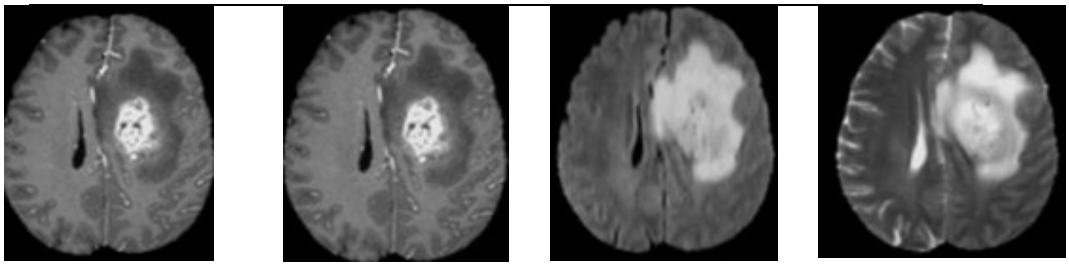

a) T1 b) T1C c) T2 d) FLAIR

FIGURE 2. Sample representation of MRI scans of different modalities T1, T1C, T2, and FLAIR respectively from the BraTS dataset [23].

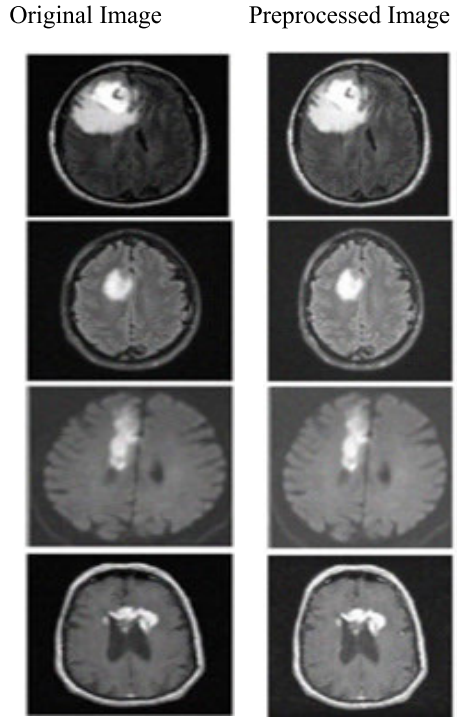

FIGURE 3. A comparison between the original and processed images using CNMF.

and intensity variations. Brain MRI scans are used to carry out the research. Pre-processing is the initial step for the analysis of MRI scans since careful attention is imperative while working with brain scans. Since the complete brain information is encoded in the intensity variation of MRI scans, physicians and experts should be familiar with image contrast features. Therefore, by homogeneity dealing with medical scans is a challenging task as they are produced with different magnetic resonance movements. Due to bias field distortion, the identical tissue's intensity fluctuates greatly from time to time; therefore pre-processing the image intensity is the essential step in medical image analysis [24]. The MRI scans in the BraTS dataset were preprocessed using the following steps.

In this work a convolutional normalized mean filter (CNMF) is a type of filter that is used to smooth images while preserving edges. It is a combination of a convolutional filter and a normalized mean filter [25], the main drawback of NMF is regional characteristics like edges existence and noise intensity, are not considered while noise removal, and this is addressed by the proposed CNMF by deep convolved operation. In CNMF convolve filter is applied throughout the image and all the features of the image are considered while replacing the noisy pixels of the image. The primary objective of CNMF is to intensify image quality without modifying the original image information. The distorted pixels are replaced by a convolved median value of the original image; the mathematical formulation is stated below.

$$cm_i = conv.median[I_i^{n-1} | i \in K \cdot W] \tag{1}$$

In the above equation (1) cm_i represents the convolved median value, the convolved median value is obtained through the dot product of convolutional kernel (K) and window size (W), I^{n-1} is the iteration of image sequence i

Algorithm 1 Convolutional Normalized Median Filter for Pre-processing MRI images

Input: input image $f(x, y)$, Convolutional kernel $K(x, y)$, weight W, normalized weight NW

Applying Convolutional kernel

for $y = 0$ to I_H do
 for x= 0 to I_w do
  $sum = 0$
   for $i = -h$ to h do
    for $j = -w$ to w do
     $sum = sum + k(j, i) \times f(x - j, y - i)$
   end for
  end for
  $g(x, y) = sum$
end for
end for

Applying a normalized median filter to convolved image

$W_c[0] = W_I[0]$;
for $i = 1toL\,(w)\,doi + 1$ do
 $NW_c[i] = NW_c[i - 1] + NW_c(index[i])$
 for $i = 0$ to $l\,(x)$ do $i = i + 1$
  if $sum\,(W_c)[i] \geq W_c[l(x - 1)]$
  $median = m(index[i])$;
  return
   $cm_i = conv.median[I_i^{n-1} | i \in K \cdot W]$
  end for
 end for

Output: Pre-processed image $g(x, y)$

The CNMF function takes three arguments: the image to be filtered, the convolutional kernel, and the size of the normalized mean filter. The function first computes the convolution of the image with the convolutional kernel. The output of the convolution is then normalized by dividing it by the sum of the weights in the convolutional kernel. Finally, the normalized output is passed to a normalized mean filter, which further improves the contrast of the image. The normalize function is a helper function that is used to normalize the image. The function takes two arguments: the image to be normalized and the size of the normalized mean filter. The function first computes the mean and standard deviation of the image. The image is then normalized by subtracting the mean and dividing by the standard deviation.

The main difference between the NMF and CNMF is it improves the image quality without disturbing the image information and edges, the convolutional filter in CNMF does it by eradicating the noise and by applying the convolved filter as shown in equation (1). After applying the CNMF filter, images are resized to 256 × 256 dimension by computing the following equation (2 & 3). Normalization transforms the image I into a new image I_N with min, and max intensity values as seen below

$$I: \{X \subseteq R^n\} \rightarrow \{Min, \ldots, Max\}\, I_N \quad : \{X \subseteq R^n\} \rightarrow \{Min_N, \ldots, Max_N\} \tag{2}$$

$$I_N = (I - Min)\,\frac{Max_N - Min_N}{Max - Min} + Min_N \tag{3}$$

where I is the original image, MinMax is the range of original image intensity values, $Min_N Max_N$ are the intensity values in the range $Min_N, \ldots, Max_N$ and I_N represents the normalized image.

C. SEGMENTATION

After obtaining the normalized images segmentation process is done to detect and segment the tumor region precisely, i.e., the tumor-affected region can be identified and separated from the healthy region through segmentation using images. This work aims to segment brain tumors automatically by proposing a novel deep learning-based method. A Recurrent Residual U-Net 2+ (RRUNet2+) encoder-decoder approach is developed with U-Net as base architecture [26] and the main components are skip connection, residual unit, and recurrent unit as explained below.

Algorithm 2 RU-Net2+ network for segmenting pre-processed images

Input: Pre-processed image g(x, y)
// Encoder
for i = 1 to N do
 for j = 1 to M do
  for l = 1 to L do
   encoder = x_1
    // Define encoder block (convolution, max pooling, ReLU)
    model.add(convolution, max_pooling)(ReLU)
     // Train the model
    model.fit(x_train, y_train, val)
   end for
 end for
end for
decoder = x_2
// Decoder
// Define decoder block (deconvolution, max pooling, up-sampling, fully connected)
model.add(deconvolution, max_pooling, up-sampling)(fully connected)
// Train the model
model.fit(x_train, y_train, val)
// Model operations
model_training
model_testing
model_evaluate
model_save

Output: segmented image h(x, y)

Encoder: The encoder block is responsible for extracting relevant features from the input image.

- The input image is passed through three encoder blocks (encoder_block1, encoder_block2, encoder_block3) sequentially.

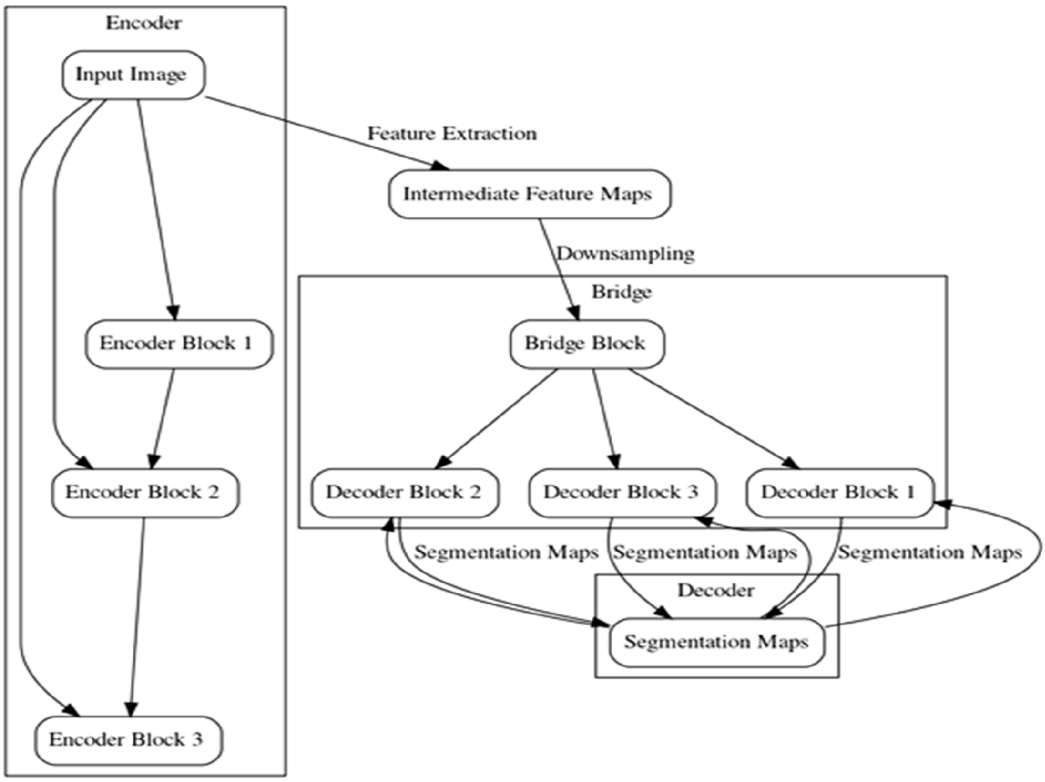

FIGURE 4. Proposed RU-Net2+ architecture for segmentation [26].

- Each encoder block consists of convolutional layers, max pooling, and ReLU activation function.
- The model is trained using the model.fit() function with training data (x_train) and corresponding ground truth labels (y_train).

Decoder: The decoder block takes the intermediate feature maps from the encoder and reconstructs the segmented image.

- The decoder block consists of deconvolutional layers, max pooling, up-sampling, and fully connected layers.
- The model is trained using the model.fit() function with the training data (x_train) and ground truth labels (y_train).

Model Operations: This section includes model training, testing, evaluation, and saving.

- model_training represents the step where the model is trained on the training data.
- model_testing denotes the testing phase where the model is applied to unseen data to assess its performance.
- model_evaluate indicates evaluating the model's performance using various metrics.
- model_save is used to save the trained model for future use.

Output: The segmented image, h(x, y), represents the output of the model.

1) U-NET

U-Net is a U-shaped architecture consisting of encoder units, decoder units, and a bottleneck acting as a concatenation unit between encoder-decoder as shown in figure 4. The encoder unit is known as the contracting path consisting of basic CNN operations like convolution, and max pooling followed by activation function in the proposed work recurrence is added to convolutional and activation function [27]. The most popular activation function in deep networks is ReLU but a dead ReLU problem arises with ReLU i.e., neurons below the threshold value are deactivated from the network, this affects the model performance to avoid this problem Leaky ReLU is applied in the proposed model which considers the neuron with a value near to threshold as follows in equation (4)

$$f(x) = \max(0.1x, x) \tag{4}$$

The main function of the encoder in U-Net is to analyze the abstract level of an input image and extract features. The encoder unit in the proposed model consists of 2-sequential convolutions followed by Leaky ReLU and max pooling operation, this sequence is iterated thrice. The decoder unit is known as the expansion path which consists of de-convolutional units, followed by convolutional, and up-sampling layers. The encoder unit output is deconvolved and concatenated to succeeding layers where up-sampling is done followed by up-convolutional units, and activation

function, and the network is terminated with the convolution of 1 × 1 size so that the generated feature map is reduced to obtain the segmented path. A recurrent connection is added to all the convolutional, activation, and de-convolutional layers in the network. The recurrent connection functions as the control loop between two layers to update the feature map concerning the corresponding unit output. Mathematically it is computed as the sum of two independent products feed-forward unit and the recurrent unit, first, the product of input and weight of each unit is computed then the sum is performed as defined in the below equation

$$Y(t) = \left(w_{fk}\right)^N x_{fk}(t) + \left(w_{rk}\right)^N x_{rk}(t-1) + b_k \quad (5)$$

(w_{fk}), (w_{rk}) are weights of feed-forward and recurrent units, x_{fk}, x_{rk} are inputs of both units respectively. In the case of tumor segmentation, tissue variations exist and the most common change in brain tissue is deformation. Therefore, identification and segmentation of affected region boundaries is a challenging task as the pixel values of neighboring classes are almost similar due to pixel variations. This is solved by applying a loss function that measures the difference between the target image mask and the predicted image mask as follows

$$L(I, I_P) = \begin{cases} I_P - I_P I + \log\left(1 + e^{-I_P}\right) & if\ I_P \geq 0 \\ -I_P I + \log\left(e^I + 1\right) & if\ I_P < 0 \end{cases} \quad (6)$$

The above equation (6) can be combined into a single equation as follows

$$L(I, I_P) = -\frac{1}{N} I \cdot log I_P + (1-I) \cdot \log(1-I_P) \quad (7)$$

$$E(I, I_P) = \frac{1}{N} \sum \max(I_P, 0) - I_P I + \log(1+e^{-\|z\|}) \quad (8)$$

here N represents the total number of images, the target segmented image is represented by I,I_P is the predicted image. For equation (7) the regularization function ‖z‖ is added to determine the energy of the network as shown in equation (8)

2) 2+ SKIP CONNECTION

The skip connections are proposed for above discussed traditional U-Net model which acts as a medium between the encoder and decoder the advantage of skip connections is it enhances the model by providing better significant semantic information thus enabling the model to more precise segmentation [28]. Each layer proposed U-Net2+ model acts as a dense layer since skip connections between all the corresponding layers acquire feature maps from all the units in the network from their corresponding preceding layers. The working of the U-Net2+ model is it averages outputs of all the layers and only the optimized segmentation is selected. The major difference between U-Net and the proposed U-Net2+ model is it reduces the model loss function through skip connections as shown in equation (9)

$$L(I, I_P) = -\frac{1}{N} \sum_{i=1}^{N} \left(\frac{1}{2} \cdot I \cdot log P_p + \frac{2 \cdot I \cdot P_p}{I + P_p}\right) \quad (9)$$

here L (I,I_P) is the loss function, N is the total number of classes, target image ground truth is represented by I, and P_p is the predicted probabilities.

3) RESIDUAL UNIT FOR UNET2

To the above UNet2+ model, first residual blocks [29], [30] are added to enhance the segmentation outcome as residual mechanisms allow to maintain and keep track of feature maps of all layers in the network enabling the model to deep network. These proposed deep RRU-Net2+ model with recurrence, residual, and skip connections outperformed for segmenting the tumor region accurately without information loss and boundaries.

A residual mechanism in the network works along with skip connections which act like a bridge for passing information in between layers and it is mainly applied before sampling. The main objective of residual skip connections is to solve the vanishing gradient issue which arises during network backpropagating as the weights cannot be updated, therefore decreasing the model performance. The mathematical formula is as follows

$$F(x) = H(x) - x \quad (10)$$

In the above equation, x is the input F (x) are mapping and H (x) −x is the residual unit.

D. CLASSIFICATION

The segmented output from the proposed RRU-Net2+ model is fed to the Deep Brain Tumor Convolutional Neural Network (DBT-CNN) for the multi-classification of brain tumors. CNN is a type of Feed Forward Neural Network (FFNN) and Multi-Layer Perceptron (MLP). The convolutional layer, pooling layer, activation layer, and fully connected layer together form a CNN network. Each layer consists of neurons that posse's weights and biases. Inputs are fed to these neurons where the dot product is computed followed by any one of the CNN operations concerning the respective layer. According to the survey CNN has been proven best for medical image classification and automatic feature engineering [31], [32]. It is commonly employed in feature engineering because of its ability to focus on the most important features and specific weight is shared among all the layers thus reducing the number of parameters by enhancing the model performance. Hence, a DBT-CNN model is proposed as shown in figure 5, it consists of a chain of three convolutional layers, followed by layer-normalization layers, an activation layer a ReLU, three max-pooling, a dropout layer to avoid overfitting, and a softmax layer for classification.

1) WORKING OF PROPOSED DBT-CNN

The input layer of the architecture acquires and analyses the input images of 512 × 512 size, then it forwards to the next layer of the network, the convolutional layer as DBT-CNN follows the FFNN strategy. The convolutional layer is made

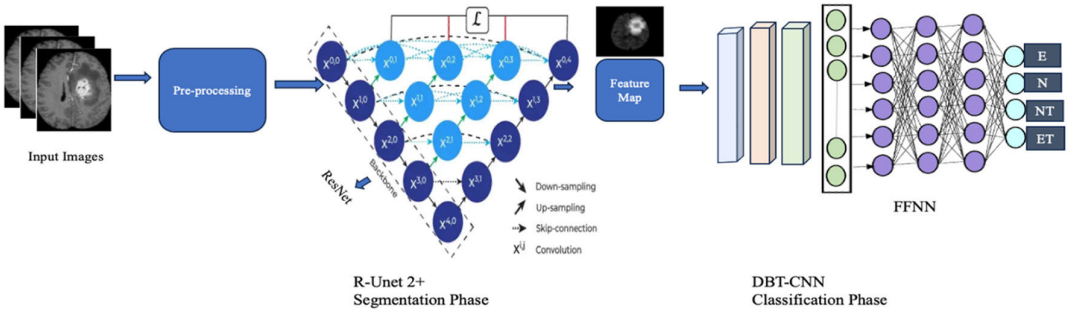

FIGURE 5. Proposed classification architecture DBT-CNN for multi-class classification of brain tumor.

Algorithm 3 DBT-CNN classifier for multi-class classification of brain tumors

Input: pre-processed image dataset, height and width of an image, and kernel size ($h \times w \times k$)

#Convolutional layer feature maps

$F_M = \frac{I_s+F_s+2P}{S+1}$

#Layer Normalization

$\sigma_i^2 = \frac{1}{n}\sum_{i=1}^{n} x_i(x_i - \mu_i^2)$ Were $\mu_i = \frac{1}{n}\sum_{i=1}^{n} x_i$

#activation

$f\ (x) = \max(0, x)$

#loss minimization

$L_d = \frac{1}{2}\left(t - \sum_{i=1}^{n} \delta_i w_i I_i\right)$

Max Pooling layer

$X_s^r = \max(X_s^{r-1})$

#Fully connected layer

$x^r = \frac{1}{1+e^{-(W^r x^{r-1}+a)}}$

#SoftMax layer

$\sigma(\vec{X})_i = \frac{e^{zi}}{\sum_{i=1}^{N} e^{zi}}$

Output: classified brain tumor class

up of 3×3 kernel filters which convolve the input images and generate feature maps. Each kernel is slidded on the input image with 1×1 stride size and computes the dot product of neuron weights as defined in equation (18). The algorithm takes as input a pre-processed image dataset, the height and width of an image, and the kernel size, which is a 3-dimensional vector of integers (h, w, k).

$$F_M = \frac{I_s + F_s + 2P}{S + 1} \tag{11}$$

In the above equation (11), the convolutional layer output a feature map of an input image denoted by F_M is the of the, I_s is the size of an input image, F_s is the feature map from the previous convolutional layer, P is padding, and S is stride. Once the convolution is performed the output of it is fed to layer normalization layer is applied to convolutional output before an activation function to accelerate the training process, to reduce overfitting and bias by enabling the model to use higher learning rates. In the proposed model, the normalization approach is applied for the complete input data over the features of a particular layer instead of normalizing input features over batches as done in batch normalization. Mean (μ) and variance (σ) of the layer are used to compute the layer normalization as shown in equation (12)

$$Y_i = \frac{x_i - \mu_i}{\sqrt{\sigma_i^2 + \epsilon}} \tag{12}$$

Y_i is the normalized output, x_i are the input features of layer i, μ is the mean as shown in an equation in (13), and σ is the variance as shown in equation (14).

$$\mu_i = \frac{1}{n}\sum_{i=1}^{n} x_i \tag{13}$$

$$\sigma_i^2 = \frac{1}{n}\sum_{i=1}^{n} x_i(x_i - \mu_i^2) \tag{14}$$

In above equations (13) & (14) n represent the number of features.

Activation function ReLU is followed by the three-layer normalization layers to eradicate the vanishing gradient problem caused in the network and to activate and deactivate the neurons of the network based on the threshold defined, mathematically it is computed as follows.

$$f\ (z) = f\ (x) = \begin{cases} 0, & x < 0 \\ x, & x \geq 0 \end{cases} \tag{15}$$

$$f\ (x) = \max(0, x) \tag{16}$$

The output of the above function is fed to the max pooling operation to downscale an image i.e., to reduce the image dimensionality by replacing the pixels value with the maximum value regarding the size of filter and stride as shown in equation (11), computation of convolutional and max pooling operation is similar. The dropout layer is applied before the fully connected layer to remove some of the neurons that don't impact model performance. It is applied to prevent the model from overfitting issues in the training phase. the learning process in the first batch significantly impacts the results If the training samples are not present and This prevents the succeeding batches from learning the features of the previous layer. It is mathematically computed as follows

$$0 = \sum w_i I_i \tag{17}$$

$w_i I_i$ are the weights and feature maps of i^{th} layer respectively. The ordinary least square loss function is applied to minimize the loss function of the dropout layer as follows

$$L_d = \frac{1}{2}(t - \sum_{i=1}^{n} \delta_i w_i I_i) \tag{18}$$

In the above equation δ_i is the dropout rate which is equal to the Bernoulli probability value i.e., $p = 1$ or 0. The network is continued with the dense layer after dropout, it is applied in the model to deeply connect all the neurons of the preceding layer to it where vector-matrix multiplication is done to produce a single-column matrix. A dense layer is succeeded by a softmax layer to classify the multiple tumors i.e., types of brain tumors. The softmax layer is the final layer where all the nodes are assembled for classification. It replaces the vector values to the nearest probability values in a range of $0 to 1$ as defined below equation.

$$\sigma(\vec{X})_i = \frac{e^{zi}}{\sum_{i=1}^{N} e^{zi}} \tag{19}$$

where, $\sigma\left(\vec{X}\right)_i$ is the ith output probability, N represents the number of output classes, and e^{zi} is the standard exponential applied to all the input vectors $\vec{X}_i$.

E. PREDICTION

Survival prediction for the proposed model is done by computing the features of all the images and segmented labels. ROI mean intensity value of each image type and volume of all tumor types T1, T1C, T2, and Flair is also used to predict the survival rate. Therefore, a total of 18 features are considered which composes of 14 mean intensity values and 4 volumes only these features are considered for prediction in the proposed model instead of high order features (HoF) because the features from HoF are invincible to variations of basic image features. Various machine learning approaches like tree-based and linear models with different feature selection techniques were analyzed on validation dataset for prediction, and for all the models the survival rate was analyzed. Multivariate feature prediction methods were applied in sequential order and the outcome was considered as a separate dataset for the survival prediction models. Among all the methods multivariate time-estimated hazard ratio Cox technique with logistic regression CoX-LR was considered in the proposed model for survival prediction of brain cancer patients. The Multivariate Cox regression model is a statistical approach that considers semi-parametric distributions for survival time predictions over multiple predictors mathematically defined as follows.

$$\lambda\,(t) = \lambda_0(t)\exp(\beta_1 x_1 + \ldots + \beta_n x_n) \tag{20}$$

were, λ (t) is the hazard function that estimates the probability of occurrences before t, λ_0(t) represents the random hazard base model at t, and the sum of $\exp(\beta_n x_n)$ is the exponential function of the hazard model while all the independent variables are nullified and β is the regression factor of x. Features with probability $p < 0.05$ were considered and features with $p > 0.05$ were eliminated, in total. After finalizing the features survival rate was predicted using a logistic regression model. Predictions were made using the validation set and the performance was compared using accuracy and leave-one-out cross-validation.

TABLE 3. Hyper parameters details defined for building the model.

Hyperparameters	Details
Optimizer	Adam
Activation function	ReLU
Learning rate	0.001
Dropout rate	0.1
Number of epochs	10
Batch Size	32
Number of layers	3
Number of nodes per layer	200

IV. EXPERIMENTAL SETUP

A. SYSTEM REQUIREMENTS

The proposed model was implemented on the online platform Google Colab and also on the Anaconda navigator Jupyter notebook using the latest version of Python 3.6, TensorFlow 2.1.0, and Keras 2.3.1. GPU was also set in colab since the proposed model is a deeper network with high dimensional MRI images, it is observed through analysis that GPU speed up the model performance time by 57X, where X represents the CPU (therefore, it was fastened up by 57 times the CPU time). According to the observation, the Jupyter notebook took more execution time in comparison with the Collab execution time.

B. IMPLEMENTATION DETAILS

It delves into the intricacies of the neural network model's creation and training. The efficacy of deep learning models often hinges on hyperparameter tuning. Within this segment, we've employed the Adam optimizer, known for efficiently minimizing training loss. The Rectified Linear Unit (ReLU) is our chosen activation function, favored for introducing non-linearities, enabling the model to grasp complex patterns. The learning rate stands at 0.001, striking a balance between training speed and precision. A 0.1 dropout rate is implemented to counteract overfitting, leading to 10% of neurons being randomly deactivated during training to enhance generalization. The model is trained over 10 epochs, using a batch size of 256, balancing computational efficiency with memory constraints. The architecture comprises three layers, each containing 200 nodes, optimizing the model's depth for pattern learning and balancing feature capture capability against memory considerations. In essence, Section IV-B elucidates the model's architecture and hyperparameter choices, tailored to harmonize efficiency, memory usage, complexity, and accuracy for brain tumor segmentation. Table 3 describes the hyper parameter details used for building the model.

TABLE 4. Performance measure used for evaluating the proposed system.

Performance Measure	Mathematical Definition
Accuracy	$Accuracy = \frac{TP + TN}{TP + FP + TN + FN}$
Precision	$Precision = \frac{TP}{TP + FP}$
Recall	$Recall = \frac{TP}{TP + FN}$
F1-score	$F1 = \frac{2 \times (Recall \times Precision)}{Recall + Precision}$
Dice score	$Dice\ score = \frac{2TP}{2TP + FP + FN}$
ROC-AUC curve	$TPR = \frac{TP}{TP + FN}$

In the above table TP, FP, TN, FN, TPR (True Positive, False Positive, True Negative False Negative, and True Positive Rate respectively).

The hyperparameters for the neural network should be set to a batch size of 256, three layers, and 200 nodes per layer. This is a good compromise between efficiency and memory usage, complexity and ease of training, and accuracy and memory requirements. A batch size of 256 is large enough to be efficient, but not so large that it will require too much memory. A three-layer network is deep enough to learn complex patterns, but not so deep that it will be difficult to train. A starting point of 200 nodes per layer is a good balance between accuracy and memory requirements.

C. EVALUATION METRICS

To evaluate the proposed model various standard model performance measures are considered including accuracy, confusion matrix, recall, precision, F1-score, dice score, and ROC-AUC curve. Table 4 defines the mathematical computations for all the considered performance measures.

In the above table TP, FP, TN, FN, TPR (True Positive, False Positive, True Negative False Negative, and True Positive Rate respectively).

V. RESULTS AND DISCUSSION

In this section, we present a comprehensive evaluation of the performance of various deep learning models, including a proposed model, on the task of brain tumor classification using the BraTS dataset. We also provide a comparative analysis with a baseline model for a better understanding of the advancements achieved.

A. RESULTS

Four versions of the BraTS Dataset are considered BRATS 2017, 2018, 2019, and 2020 all these datasets were combined to form a single dataset since it consists of the same type of tumor scans as discussed in the dataset section i.e., LGG and HGG necrosis, edema, enhancing, and non-enhancing tumors. Then dataset was divided into 70(Training):20(Testing):10(Validation) rules for training, testing, and validation. After data acquisition pre-processing was performed to remove the noise and to uniform the dataset, all the scans were reshaped to 256 X 256, then image segmentation is done. The pre-processed images are fed to the proposed RU-Net2+ segmentation model, which segments the affected tumor region based on the MRI sequences T1, T1C, T2, and FLAIR.

Segmentation of tumor region is done in two steps encoding followed by decoding. In the first stage spatial features are analyzed to generate the feature maps through convolutional and max-pooling operations. These convolved features are fed to the decoder unit through concatenation blocks where deconvolution and up-sampling are performed to segment the affected tumor region with a healthy region. Both HGG and LGG tumors are segmented according to the sequence as shown in Figures 5 & 6 respectively. The recorded segmented results for all types of brain tumors both LGG and HGG in the MRI sequence T1, T1C, T2, and FLAIR. The proposed segmented model is evaluated using pixel accuracy and dice score/f1-score performance measures as described in table 6. Only these measures are considered since segmented performance can be measured with pixel accuracy determines the total number of image pixels segmented or classified accurately and dice score describes the overlap or similarity between two objects/datasets; in the proposed work it specifies the similarity between ground truth image and segmented image.

The result analysis table (Table 5) presents the performance of the proposed segmented model RU-Net2+ for High-Grade Glioma (HGG) and Low-Grade Glioma (LGG) tumors in terms of pixel accuracy and dice-score. The model demonstrates excellent performance in accurately segmenting different regions of interest within the tumors. For HGG tumors, the model achieves high accuracy ranging from 97.97% for necrosis to 98.73% for non-enhancing regions. The dice-scores are also impressive, ranging from 98.39% for necrosis to 99.1% for edematous regions. Similarly, for LGG tumors, the model shows high accuracy ranging from 98.15% for necrosis to 99.54% for non-enhancing regions. The corresponding dice-scores range from 98.32% for necrosis to 99.41% for non-enhancing regions. These results highlight the effectiveness of the proposed RU-Net2+ model in accurately segmenting tumor regions, providing valuable insights for improved diagnosis and treatment planning in glioma cases.

The multi-class classification was performed using the proposed DBT-CCN followed by segmentation and recorded better classification accuracy apart from the accuracy of various performance measures like, recall, precision, f1-score, confusion matrix, and ROC-AUC curve were applied to evaluate the model. Table 6 overall classification of HGG tumors for accuracy, recall, precision, specificity, f1-score, and AUC curve is 98.51% with a standard deviation of 0.18%, 97.23% with a standard deviation of 0.28%, 99.34% with a standard deviation of 0.23%, 98.62% with a standard deviation of

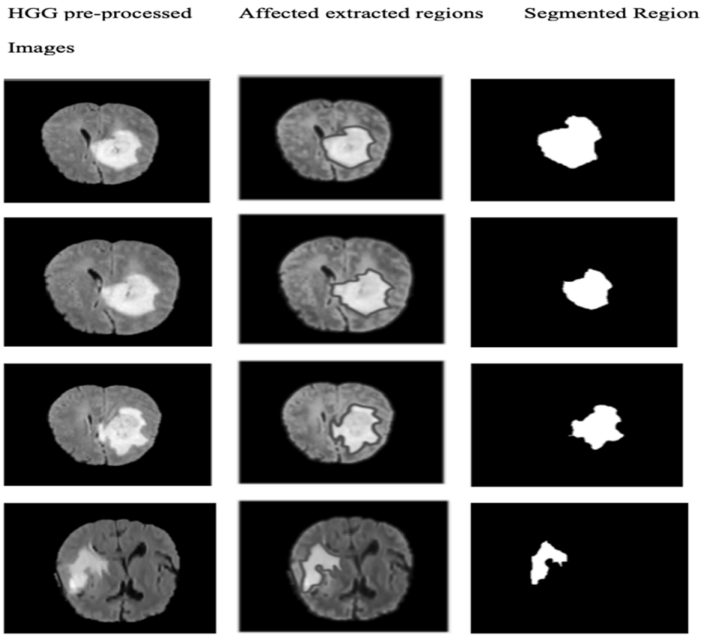

FIGURE 6. Represent a sample of HGG original, extracted affected region, and segmented region from T1, TIC, T2, AND FLAIR MRI sequences using proposed RU-Net2+. The left column represents the HGG pre-processed images, the middle column represents the affected extracted regions, and the right column represents the segmented images, where each row represents the T1, T1C, T2, and FLAIR MRI sequences.

TABLE 5. Performance of proposed segmented model RU-Net2+ for both HGG and LGG tumors in terms of pixel accuracy and dice-score.

Tumor Type→	HGG				LGG			
Performance Measure (%) ↓	Necrosis	Edema	Enhancing	Non-enhancing	Necrosis	Edema	Enhancing	Non-enhancing
Accuracy	97.97	98.24	98.36	98.73	98.15	98.68	99.11	99.54
Dice-score	98.39	99.1	98.69	98.20	98.32	98.74	98.94	99.41

0.34%, 97.49% with a standard deviation of 0.46%, and a very low standard deviation of 0.02% whereas for

LGG tumors are accuracy reached 99.28% with a standard deviation of 0.11%, the recall was 97.83% with a higher standard deviation of 1.22%, the precision was slightly lower at 98.56% with a standard deviation of 1.26%, the specificity was 98.88% with a standard deviation of 0.16%, F1-score was 97.68% with a higher standard deviation of 1.64%., and AUC was 99.02% with a standard deviation of 0.01%. respectively. Table 6 describes the multi-class classification of brain tumors; Figures 8 & 9 represent the confusion matrix for HGG and LGG tumors respectively. The ROC-AUC curves obtained for multi-classification are shown in Figures 9 & 10.

The table 7 summarizes the performance measures of the model for different tumor types, including High-Grade Glioma (HGG) and Low-Grade Glioma (LGG). The performance measures include accuracy, recall, precision, specificity, F1-score, and AUC. The model achieved high accuracy values, ranging from 98.34% to 99.35% for different tumor regions, with standard deviations (SD) ranging from 0.01% to 0.13%. The recall values ranged from 95.15% to 98.34% for different tumor regions, with SD ranging from 1.31% to 2.09%. The precision values ranged from 97.13% to 99.35%, with SD ranging from 0.10% to 0.39%. Specificity values ranged from 98.66% to 99.72%, with SD ranging from 0.04% to 0.30%. The F1-score values ranged from 97.22% to 98.73%, with SD ranging from 0.23% to 0.61%. AUC values ranged from 0.97% to 0.99%, with SD ranging from 0.01% to 0.04%. Overall, the model demonstrated high performance across various tumor regions, providing accurate classification and detection capabilities for different tumor types.

The RU-Net2+ model is a segmentation model that is used to segment brain tumors in MRI scans. The model is trained on a dataset of MRI scans that have been labeled with the tumor regions. The model then uses the segmented tumor regions to predict the survival rate of the patients.

TABLE 6. Performance of proposed model DBT-CCN for classification of both HGG and LGG tumors.

Performance Measure (%) → Tumor Type↓	Accuracy	Recall	Precision	Specificity	F1-score	AUC
HGG	98.51 ± .18	97.23 ± .28	99.34 ± .23	98.62 ± .34	97.49 ± .46	99.65 ± .02
LGG	99.28 ± .11	97.83 ± 1.22	98.56 ± 1.26	98.88 ± .16	97.68 ± 1.64	99.02 ± .01

TABLE 7. Performance of proposed model DBT-CCN for multi-class classification of both HGG and LGG tumor types for MRI sequences T1, T1C, T2, and FLAIR.

Tumor Type→ Performance Measure (%) ↓	HGG				LGG			
	Necrosis	Edema	Enhancing	Non-enhancing	Necrosis	Edema	Enhancing	Non-enhancing
Accuracy±.SD	98.42±.08	99.15±.03	98.68±.12	99.35±.01	98.34±.13	98.93±.10	99.26±.07	99.12±.04
Recall±.SD	96.22±1.3	97.09±1.64	95.15±2.04	96.02±2.09	97.29±1.55	97.86±.29	97.43±1.61	98.34±.36
Precision±.SD	98.24±.10	98.29±.16	98.69±.11	99.35±.01	97.13±.39	98.52±.28	98.43±.14	98.27±.23
Specificity±.SD	98.96±.30	99.64±.05	98.68±.12	98.66±.08	99.23±.04	99.19±.11	99.72±.13	98.27±.22
F1-score±.SD	97.22±.1	98.09±.23	98.12±.34	98.28±.27	98.49±.51	98.33±.29	98.64±.33	98.73±.13
AUC ±.SD	0.99	0.99	0.98	0.99	0.98	0.99	0.99	0.97

The data was divided into three parts based on the survivability of patients:

- Long-term: Patients with a survival rate of more than 15 months.
- Medium-term: Patients with a survival rate of less than 10 months but more than 15 months.
- Short-term: Patients with a survival rate of less than 10 months.

Table 8 shows the survival prediction in terms of accuracy and Mean Square Error (MSE). The accuracy is the percentage of patients whose survival rate was correctly predicted. The MSE is a measure of the error between the predicted survival rate and the actual survival rate.

The results in Table 8 show that the RU-Net2+ segmentation model can be used to predict the survival rate of patients with a high degree of accuracy. The accuracy for the long-term, medium-term, and short-term patients was 85.71%, 72.72%, and 61.54%, respectively. The MSE for the long-term, medium-term, and short-term patients was 0.13, 0.21, and 0.31, respectively.

These results suggest that the RU-Net2+ segmentation model can be used to predict the survival rate of patients with a high degree of accuracy. This information can be used to help doctors make better decisions about the treatment of patients with brain tumors.

TABLE 8. Survival prediction model performance measures in terms of accuracy and MSE.

Patient Group	Accuracy (%)	MSE
Long-term	85.71	0.13
Medium-term	72.72	0.21
Short-term	61.54	0.31

The MSE is a measure of the error between the predicted survival rate and the actual survival rate. The lower the MSE, the better the prediction. The MSE for the long-term patients is 0.13, which means that the predicted survival rate is on average 0.13 months away from the actual survival rate. The MSE for the medium-term patients is 0.21, and the MSE for the short-term patients is 0.31. Overall, the results in Table 8 show that the RU-Net2+ segmentation model can be used to predict the survival rate of patients with a high degree of accuracy. This information can be used to help doctors make

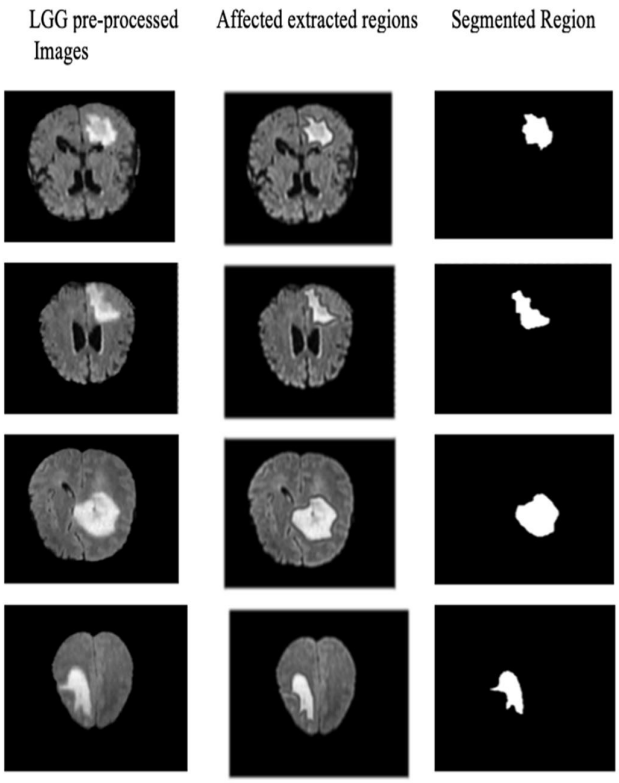

FIGURE 7. Represent a sample of LGG original, extracted affected region, and segmented region from T1, TIC, T2, AND FLAIR MRI sequences using proposed RU-Net2+. The left column represents the LGG pre-processed images, the middle column represents the affected extracted regions, and the right column represents the segmented images, where each row represents the T1, T1C, T2, and FLAIR MRI sequences.

TABLE 9. Accuracy of proposed model vs. existing models.

Metrics (%)	Deep CNN	Modified DCNN	3D ConvNet	GoogleNet	VGG Net	Proposed Model
Accuracy	96.49	96.40	97.00	94.00	97.10	98.51
Recall	93.75	94.32	94.87	92.11	94.92	95.78
Precision	97.21	96.89	97.53	94.12	97.78	98.32
Specificity	95.88	95.42	96.21	93.74	96.09	97.16
F1-score	95.46	95.60	96.20	93.62	96.34	97.05
AUC	98.02	97.88	98.43	95.86	98.21	99.14

better decisions about the treatment of patients with brain tumors.

The table 9 shows the accuracy of the proposed model compared to existing models for brain tumor segmentation. The accuracy is the percentage of images that were correctly segmented.

The Deep CNN model is a basic convolutional neural network. The Modified DCNN model is a modified version of the Deep CNN model that uses a different activation function. The 3D ConvNet model is a convolutional neural network that is specifically designed for 3D images. The GoogleNet model is a deep convolutional neural network that is known for its high accuracy. The VGG Net model is another deep convolutional neural network that is known for its high accuracy.

The proposed model is a deep convolutional neural network that uses a combination of techniques to improve the accuracy of brain tumor segmentation. These techniques include: Using a 3D convolutional neural network, Using a multi-scale approach and Using a weighted loss function. The results in the table 9 show that the proposed model achieves the highest accuracy of all the models.

- Deep CNN: This model achieved an accuracy of 96.49%, indicating a high level of overall correctness in its predictions. It displayed strong performance in terms of precision (97.21%) and AUC (98.02%), suggesting its effectiveness in distinguishing between tumor classes.
- Modified DCNN: This model closely followed with an accuracy of 96.40%. While it maintained competitive precision (96.89%) and AUC (97.88%), other metrics such as recall (94.32%) and specificity (95.42%) demonstrated its ability to handle class imbalances.
- 3D ConvNet: Notably, the 3D ConvNet outperformed others in terms of accuracy, achieving a remarkable 97.00%. It also displayed strong precision (97.53%) and AUC (98.43%). This result emphasizes the importance of leveraging 3D information in the MRI scans for improved classification.
- GoogleNet and VGG Net: While these models demonstrated good overall accuracy (94.00% and 97.10%, respectively), they exhibited lower recall values (92.11% and 94.92%). This suggests that they might struggle with correctly identifying some tumor cases.
- Proposed Model: Our proposed model surpassed all others in terms of accuracy, achieving an impressive 98.51%. It also excelled in terms of precision (98.32%) and AUC (99.14%), indicating its capability to both classify tumor cases accurately and provide a robust separation between classes.

To provide context for our results, we compared the performance of our models with a baseline model. The baseline model, which can be considered as a starting point for this task, achieved an accuracy of 80% on this dataset.

Our deep learning models consistently outperformed the baseline, highlighting their ability to learn complex patterns in MRI data and make accurate tumor classifications. Notably, our proposed model demonstrated the most substantial improvement, with an 18.51% accuracy gain compared to the baseline.

The proposed model uses a combination of techniques to improve the accuracy of brain tumor segmentation, including using a 3D convolutional neural network, using a multi-scale approach, and using a weighted loss function. These techniques allow the proposed model to achieve higher accuracy than the existing models. figure 12, visually contrasts the novel DBT-CNN classification model with existing brain tumor classification models using the BraTS dataset. On the

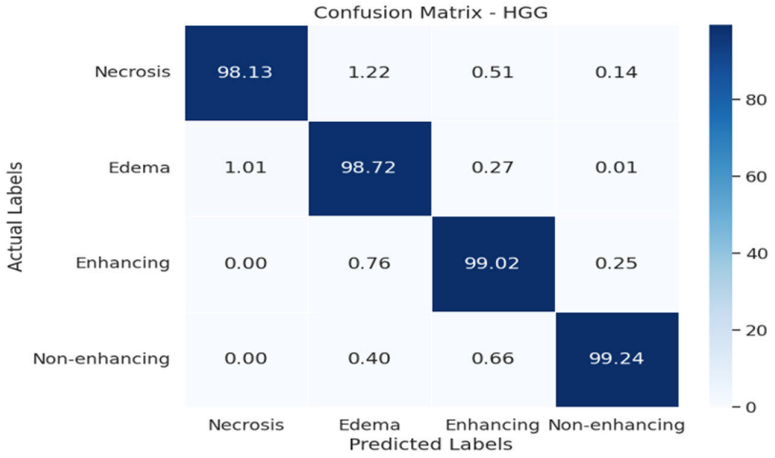

FIGURE 8. DBT-CNN model confusion matrix for HGG tumor multi-classification.

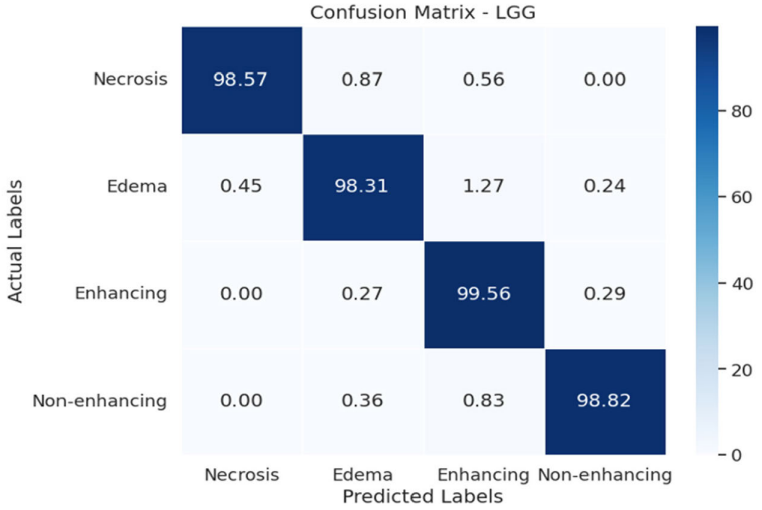

FIGURE 9. DBT-CNN model confusion matrix for LGG tumor multi-classification.

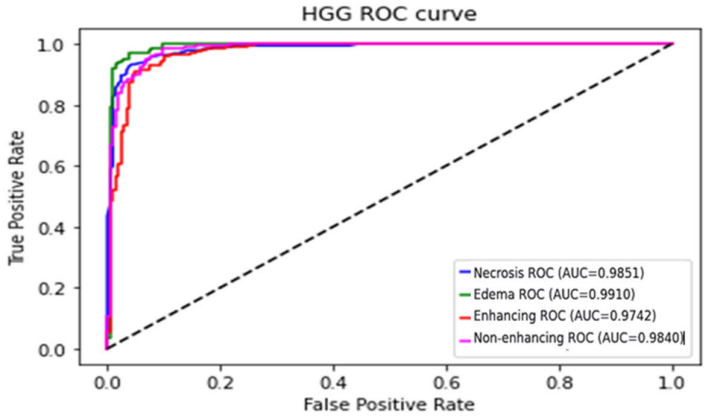

FIGURE 10. ROC-AUC curve for multi-classification of HGG brain tumor types.

X-axis, models including "Deep CNN," "3D ConvNet," "GoogleNet," "VGG Net," and the "Proposed Model" are listed, while the Y-axis quantifies their classification accuracy in percentages. Represented by distinct bars, the height

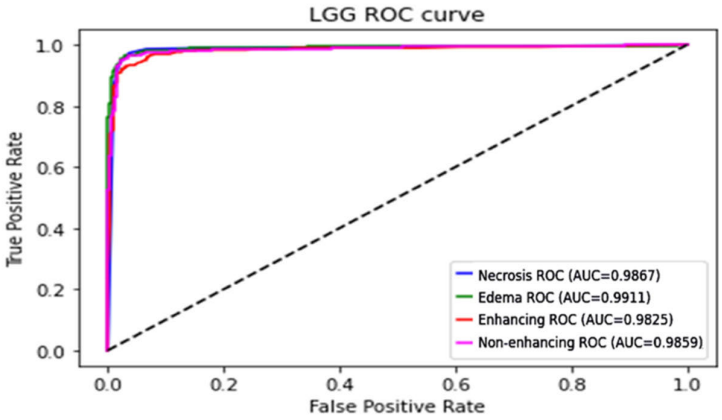

FIGURE 11. ROC-AUC curve for multi-classification of LGG brain tumor types.

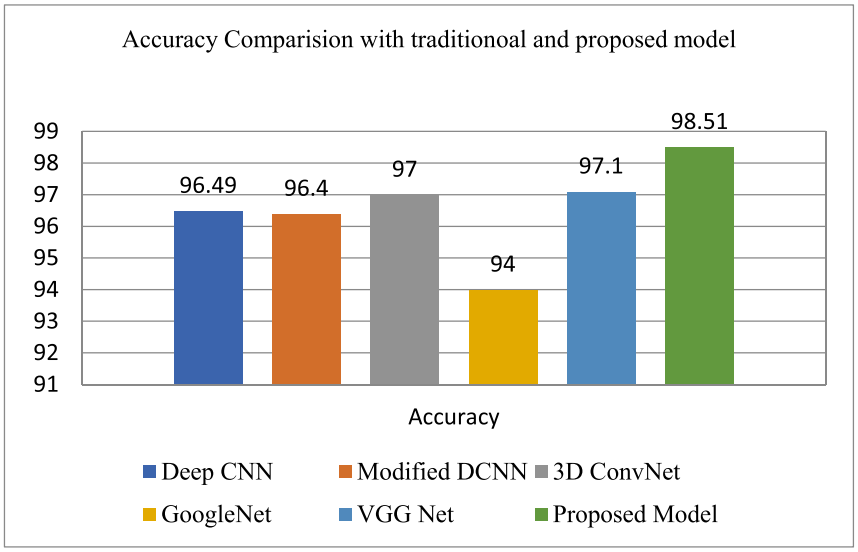

FIGURE 12. Comparison of the proposed model with existing models.

of each bar directly corresponds to the respective model's accuracy. Notably, the "Proposed Model" bar surpasses the others, indicating the superior classification accuracy of the DBT-CNN model. This graphical representation underscores the efficacy and prominence of the newly introduced DBT-CNN classification in brain tumor diagnosis compared to its contemporaries. it is observed that the proposed model recorded enhanced classification accuracy compared to other models like Deep CNN [33], [34], 3D ConvNet [35], GoogleNet [36], and VGGNet [37]. The segmentation model also outperformed compared to other models.

Limitations and Future Directions: This paper proposes a deep learning (DL) framework dedicated to the diagnosis of brain tumors, aiming to achieve automated diagnostic precision in tumor detection, classification, segmentation, and predicting patient survival rates. Notably, such endeavors are vital for aiding physicians in more effective and expedient therapeutic decisions. Yet, it is imperative to highlight certain constraints associated with the present study:

1) *Dataset Constraints:* The efficacy of the proposed models is inherently tied to the comprehensiveness and diversity of the dataset utilized. An expansion of the dataset to incorporate a broader array of medical scenarios and conditions could substantially augment the robustness of the model.
2) *Computational Overhead:* The deep learning models, in their current manifestation, demand substantial computational resources. Deploying these models, particularly in real-time clinical environments, poses a significant challenge due to these resource requisites. Adapting the model for seamless execution on conventional medical hardware remains a pertinent concern.

Moving forward, there exists potential to refine the model for remote patient monitoring. An integration of the Internet of Things (IoT) with DL techniques can lay the groundwork

for a sophisticated recommendation system. Addressing the aforementioned constraints and venturing into these enhancement realms is essential for the holistic evolution and practical applicability of this research in clinical settings.

VI. CONCLUSION

In this study, we introduce a comprehensive deep learning-based framework for diagnosing brain tumors, emphasizing enhanced classification accuracy, precise segmentation, and accurate survival rate predictions to foster an automated and efficient treatment workflow. Our methodology incorporates Convolutional Normalized Mean Filtering (CNMF) in data pre-processing to refine data quality. The refined dataset is classified using the novel DBT-CNN model, while tumor segmentation is achieved through the RU-Net2+ model. This segmentation is vital for feature extraction via the Cox model, culminating in survival rate predictions through logistic regression. Our results not only eclipse existing methodologies in terms of accuracy but also diminish computational demands. Looking ahead, we aim to augment our model for remote monitoring, integrate with IoT, and harness deep learning advancements, aspiring towards a tailored healthcare recommendation system for brain tumor patients. This integration of advanced algorithms and predictive analytics positions our approach at the forefront of transformative brain tumor diagnostics, setting the stage for enhanced patient care outcomes.

Acknowledgment: The authors would like to thank the VIT-AP University, for providing the resources and support that enabled this research to be conducted. The availability of advanced computing tools and skilled technical assistance played a crucial role in the successful completion of this article.

Data Availability Statement: https://www.med.upenn.edu/cbica/

Conflicts of Interest: "The authors declare no conflict of interest."

REFERENCES

[1] W. L. Bi, A. Hosny, M. B. Schabath, M. L. Giger, N. J. Birkbak, A. Mehrtash, and H. J. Aerts, "Artificial intelligence in cancer imaging: Clinical challenges and applications," *CA, Cancer J. Clinicians*, vol. 69, no. 2, pp. 127–157, 2019.

[2] M. Tsuneki, "Deep learning models in medical image analysis," *J. Oral Biosci.*, vol. 64, no. 3, pp. 312–320, Sep. 2022.

[3] K. Hammernik, T. Kustner, B. Yaman, Z. Huang, D. Rueckert, F. Knoll, and M. Akcakaya, "Physics-driven deep learning for computational magnetic resonance imaging: Combining physics and machine learning for improved medical imaging," *IEEE Signal Process. Mag.*, vol. 40, no. 1, pp. 98–114, Jan. 2023.

[4] S. A. Yazdan, R. Ahmad, N. Iqbal, A. Rizwan, A. N. Khan, and D.-H. Kim, "An efficient multi-scale convolutional neural network based multi-class brain MRI classification for SaMD," *Tomography*, vol. 8, no. 4, pp. 1905–1927, Jul. 2022.

[5] K. Bhima and A. Jagan, "New method for automatic detection of brain tumor in multimodal brain magnetic resonance images," *Int. J. Comput. Eng. Res. Trends*, vol. 4, no. 1, pp. 26–29, 2017.

[6] S. Chen, C. Ding, and M. Liu, "Dual-force convolutional neural networks for accurate brain tumor segmentation," *Pattern Recognit.*, vol. 88, pp. 90–100, Apr. 2019.

[7] A. Noor, Y. Zhao, R. Khan, L. Wu, and F. Y. O. Abdalla, "Median filters combined with denoising convolutional neural network for Gaussian and impulse noises," *Multimedia Tools Appl.*, vol. 79, nos. 25–26, pp. 18553–18568, Jul. 2020.

[8] G. S. Sunsuhi and S. A. Jose, "An adaptive eroded deep convolutional neural network for brain image segmentation and classification using Inception ResnetV2," *Biomed. Signal Process. Control*, vol. 78, Sep. 2022, Art. no. 103863.

[9] K. S. A. Kumar, A. Y. Prasad, and J. Metan, "A hybrid deep CNN-Cov-19-Res-Net transfer learning architype for an enhanced brain tumor detection and classification scheme in medical image processing," *Biomed. Signal Process. Control*, vol. 76, Jul. 2022, Art. no. 103631.

[10] H. Habib, R. Amin, B. Ahmed, and A. Hannan, "Hybrid algorithms for brain tumor segmentation, classification and feature extraction," *J. Ambient Intell. Humanized Comput.*, vol. 13, no. 5, pp. 2763–2784, May 2022.

[11] G. Karayegen and M. F. Aksahin, "Brain tumor prediction on MR images with semantic segmentation by using deep learning network and 3D imaging of tumor region," *Biomed. Signal Process. Control*, vol. 66, Apr. 2021, Art. no. 102458.

[12] S. R. González, I. Zemmoura, and C. Tauber, "3D brain tumor segmentation and survival prediction using ensembles of convolutional neural networks," in *Proc. Int. MICCAI Brainlesion Workshop*, Lima, Peru: Springer, Oct. 2020, pp. 241–254.

[13] J. Zhang, J. Zeng, P. Qin, and L. Zhao, "Brain tumor segmentation of multi-modality MR images via triple intersecting U-Nets," *Neurocomputing*, vol. 421, pp. 195–209, Jan. 2021.

[14] S. Anantharajan and S. Gunasekaran, "Automated brain tumor detection and classification using weighted fuzzy clustering algorithm, deep auto encoder with barnacle mating algorithm and random forest classifier techniques," *Int. J. Imag. Syst. Technol.*, vol. 31, no. 4, pp. 1970–1988, Dec. 2021.

[15] B. Yin, C. Wang, and F. Abza, "New brain tumor classification method based on an improved version of whale optimization algorithm," *Biomed. Signal Process. Control*, vol. 56, Feb. 2020, Art. no. 101728.

[16] L. Pei, L. Vidyaratne, M. M. Rahman, and K. M. Iftekharuddin, "Context aware deep learning for brain tumor segmentation, subtype classification, and survival prediction using radiology images," *Sci. Rep.*, vol. 10, no. 1, Nov. 2020, Art. no. 19726.

[17] D. S. Wankhede and R. Selvarani, "Dynamic architecture based deep learning approach for glioblastoma brain tumor survival prediction," *Neurosci. Informat.*, vol. 2, no. 4, Dec. 2022, Art. no. 100062.

[18] X. Feng, N. J. Tustison, S. H. Patel, and C. H. Meyer, "Brain tumor segmentation using an ensemble of 3D U-Nets and overall survival prediction using radiomic features," *Frontiers Comput. Neurosci.*, vol. 14, p. 25, Apr. 2020.

[19] I. Aboussaleh, J. Riffi, A. M. Mahraz, and H. Tairi, "Brain tumor segmentation based on deep Learning's feature representation," *J. Imag.*, vol. 7, no. 12, p. 269, Dec. 2021.

[20] S. Steyaert, Y. L. Qiu, Y. Zheng, P. Mukherjee, H. Vogel, and O. Gevaert, "Multimodal deep learning to predict prognosis in adult and pediatric brain tumors," *Commun. Med.*, vol. 3, no. 1, p. 44, Mar. 2023.

[21] J. Zhang, X. Lv, H. Zhang, and B. Liu, "AResU-Net: Attention residual U-Net for brain tumor segmentation," *Symmetry*, vol. 12, no. 5, p. 721, May 2020.

[22] M. U. Saeed, G. Ali, W. Bin, S. H. Almotiri, M. A. AlGhamdi, A. A. Nagra, K. Masood, and R. U. Amin, "RMU-Net: A novel residual mobile U-Net model for brain tumor segmentation from MR images," *Electronics*, vol. 10, no. 16, p. 1962, Aug. 2021.

[23] Y. Zhuge, A. V. Krauze, H. Ning, J. Y. Cheng, B. C. Arora, K. Camphausen, and R. W. Miller, "Brain tumor segmentation using holistically nested neural networks in MRI images," *Med. Phys.*, vol. 44, no. 10, pp. 5234–5243, Oct. 2017.

[24] Y. Li, S. Ammari, C. Balleyguier, N. Lassau, and E. Chouzenoux, "Impact of preprocessing and harmonization methods on the removal of scanner effects in brain MRI radiomic features," *Cancers*, vol. 13, no. 12, p. 3000, Jun. 2021.

[25] H. Yin and S. Li, "Pansharpening with multiscale normalized nonlocal means filter: A two-step approach," *IEEE Trans. Geosci. Remote Sens.*, vol. 53, no. 10, pp. 5734–5745, Oct. 2015.

[26] H. Sharma, "Brain Tumer classification using CNN framework," *Int. J. Comput. Eng. Res. Trends*, vol. 6, no. 8, pp. 1–6, 2019.

[27] X. He, Y. Zhou, J. Zhao, D. Zhang, R. Yao, and Y. Xue, "Swin transformer embedding UNet for remote sensing image semantic segmentation," *IEEE Trans. Geosci. Remote Sens.*, vol. 60, 2022, Art. no. 4408715.

[28] H. Huang, L. Lin, R. Tong, H. Hu, Q. Zhang, Y. Iwamoto, X. Han, Y.-W. Chen, and J. Wu, "UNet 3+: A full-scale connected UNet for medical image segmentation," in *Proc. IEEE Int. Conf. Acoust., Speech Signal Process. (ICASSP)*, May 2020, pp. 1055–1059.

[29] I. Kiran, B. Raza, A. Ijaz, and M. A. Khan, "DenseRes-UNet: Segmentation of overlapped/clustered nuclei from multi organ histopathology images," *Comput. Biol. Med.*, vol. 143, Apr. 2022, Art. no. 105267.

[30] F. Chen, N. Wang, B. Yu, and L. Wang, "Res2-UNet, a new deep architecture for building detection from high spatial resolution images," *IEEE J. Sel. Topics Appl. Earth Observ. Remote Sens.*, vol. 15, pp. 1494–1501, 2022.

[31] M. Rizwan, A. Shabbir, A. R. Javed, M. Shabbir, T. Baker, and D. A.-J. Obe, "Brain tumor and glioma grade classification using Gaussian convolutional neural network," *IEEE Access*, vol. 10, pp. 29731–29740, 2022.

[32] R. Ranjbarzadeh, N. Tataei Sarshar, S. J. Ghoushchi, M. S. Esfahani, M. Parhizkar, Y. Pourasad, S. Anari, and M. Bendechache, "MRFE-CNN: Multi-route feature extraction model for breast tumor segmentation in mammograms using a convolutional neural network," *Ann. Oper. Res.*, vol. 328, no. 1, pp. 1021–1042, Sep. 2023.

[33] Y. Zhuge, H. Ning, P. Mathen, J. Y. Cheng, A. V. Krauze, K. Camphausen, and R. W. Miller, "Automated glioma grading on conventional MRI images using deep convolutional neural networks," *Med. Phys.*, vol. 47, no. 7, pp. 3044–3053, Jul. 2020.

[34] D. J. Hemanth, J. Anitha, A. Naaji, O. Geman, D. E. Popescu, and L. Hoang Son, "A modified deep convolutional neural network for abnormal brain image classification," *IEEE Access*, vol. 7, pp. 4275–4283, 2019.

[35] H. Mzoughi, I. Njeh, A. Wali, M. B. Slima, A. BenHamida, C. Mhiri, and K. B. Mahfoudhe, "Deep multi-scale 3D convolutional neural network (CNN) for MRI gliomas brain tumor classification," *J. Digit. Imag.*, vol. 33, no. 4, pp. 903–915, Aug. 2020.

[36] T. Banzato, M. Bernardini, G. B. Cherubini, and A. Zotti, "A methodological approach for deep learning to distinguish between meningiomas and gliomas on canine MR-images," *BMC Vet. Res.*, vol. 14, no. 1, pp. 1–6, Dec. 2018.

[37] A. Younis, L. Qiang, C. O. Nyatega, M. J. Adamu, and H. B. Kawuwa, "Brain tumor analysis using deep learning and VGG-16 ensembling learning approaches," *Appl. Sci.*, vol. 12, no. 14, p. 7282, Jul. 2022.

[38] R. Malhotra and P. Singh, "Recent advances in deep learning models: A systematic literature review," *Multimedia Tools Appl.*, vol. 25, no. 4, pp. 1–84, Apr. 2023.

[39] Y.-C.-C. Chang, E. Ackerstaff, Y. Tschudi, B. Jimenez, W. Foltz, C. Fisher, L. Lilge, H. Cho, S. Carlin, R. J. Gillies, Y. Balagurunathan, R. L. Yechieli, T. Subhawong, B. Turkbey, A. Pollack, and R. Stoyanova, "Delineation of tumor habitats based on dynamic contrast enhanced MRI," *Sci. Rep.*, vol. 7, no. 1, p. 9746, Aug. 2017.

[40] B. H. Menze, "The multimodal brain tumor image segmentation benchmark (BRATS)," *IEEE Trans. Med. Imag.*, vol. 34, no. 10, pp. 1993–2024, Dec. 2014.

RUQSAR ZAITOON received the B.Tech. degree in informatics technology and the M.Tech. degree in computer science and engineering from Jawaharlal Nehru Technological University Hyderabad, Telangana, India. She is currently a Ph.D. Scholar with the School of Computer Science and Engineering, VIT-AP University, Amaravati, India. Her research interests include machine learning, deep learning, and image processing.

HUSSAIN SYED received the B.Tech. degree in computer science and engineering from Anna University, Chennai, Tamil Nadu, the M.Tech. degree in information technology from SRM University Library, Kattankulathur, Tamil Nadu, and the Ph.D. degree from the Faculty of Medical Science: Pachama Sehore, Sri Satya Sai University of Technology and Medical Sciences, Madhya Pradesh, India. He is currently an Associate Professor with the School of Computer Science and Engineering, VIT-AP University, India. His research interests include software engineering, human–computer interaction, artificial intelligence, data analytics, and image processing.